IEEE Access
Multidisciplinary ⋮ Rapid Review ⋮ Open Access Journal

Received March 14, 2020, accepted April 16, 2020, date of publication April 28, 2020, date of current version May 14, 2020.

Digital Object Identifier 10.1109/ACCESS.2020.2990881

Galileo Hand: An Anthropomorphic and Affordable Upper-Limb Prosthesis

JULIO FAJARDO[1,2], VICTOR FERMAN[2], DIEGO CARDONA[1], GUILLERMO MALDONADO[1], ALI LEMUS[1], AND ERIC ROHMER[2]

[1]Turing Research Laboratory, FISICC, Galileo University, Guatemala City 01010, Guatemala
[2]Department of Computer Engineering and Industrial Automation, FEEC, UNICAMP, Campinas 13083-852, Brazil

Corresponding author: Julio Fajardo (julio.fajardo@galileo.edu)

This work was supported in part by the FAPESP-CEPID/BRAINN under Grant 2013/07559-3, and in part by the MCTI/SECIS/FINEP/FNDCT under Grant 0266/15.

ABSTRACT The strict development processes of commercial upper-limb prostheses and the complexity of research projects required for their development makes them expensive for end users, both in terms of acquisition and maintenance. Moreover, many of them possess complex ways to operate and interact with the subjects, influencing patients to not favor these devices and shed them from their activities of daily living. The advent of 3D printers allows for distributed open-source research projects that follow new design principles; these consider simplicity without neglecting performance in terms of grasping capabilities, power consumption and controllability. In this work, a simple, yet functional design based on 3D printing is proposed, with the aim to reduce costs and manufacturing time. The operation process consists in interpreting the user intent with electromyography electrodes, while providing visual feedback through a μLCD screen. Its modular, parametric and self-contained design is intended to aid people with different transradial amputation levels, despite of the socket's constitution. This approach allows for easy updates of the system and demands a low cognitive effort from the user, satisfying a trade-off between functionality and low cost. It also grants an easy customization of the amount and selection of available actions, as well as the sensors used for gathering the user intent, permitting alterations to fit the patients' unique needs. Furthermore, experimental results showed an apt mechanical performance when interacting with everyday life objects, in addition to a highly accurate and responsive controller; this also applies for the user-prosthesis interface.

INDEX TERMS Prosthetic hand, three-dimensional printing, electromyography, user-prosthesis interface.

I. INTRODUCTION

The last World Report on disabilities shows that there are at least 30 million people with amputations residing in developing countries and most of them do not have possibilities to acquire prosthetic care, neither can they afford leading commercial assistive technology with pricing around $1000, such as upper-limb prosthetic devices [1]–[4]. Additionally, the acquisition of these assistive devices is problematic in these countries, since availability is not guaranteed [2], [3]. Meanwhile, several research laboratories focus on improving dexterity and biomimetics of prosthetic hands, as well as implementing expensive and intrusive ways to gather the user intent [5]–[9], while, sometimes, neglecting other vital aspects of the prosthetic device, like aesthetics, controllability and the user interface, the lack of which can influence patients to stop using them [10]. This phenomenon also occurs with commercial prostheses, because they require long periods of training and adaptation to aptly interact with the user-prosthesis interface (UPI), which is, commonly, powered by myoelectric controllers [11]; this can be corrected by implementing an amiable and intuitive alternative.

Because of the limitations of conventional body-powered prostheses, like steel hooks, and the elevated cost, weight and difficulties to repair commercial myoelectric prosthetic devices [12]–[14], many open-source projects based on 3D printing technologies have been released [14]–[17], whose target is a lightweight and affordable upper-limb prosthetic device. This encourages its widespread distribution through global networks by reducing manufacturing costs. That is why the implementation of said technology in assistive devices has been increasing; improving

The associate editor coordinating the review of this manuscript and approving it for publication was Jenny Mahoney.

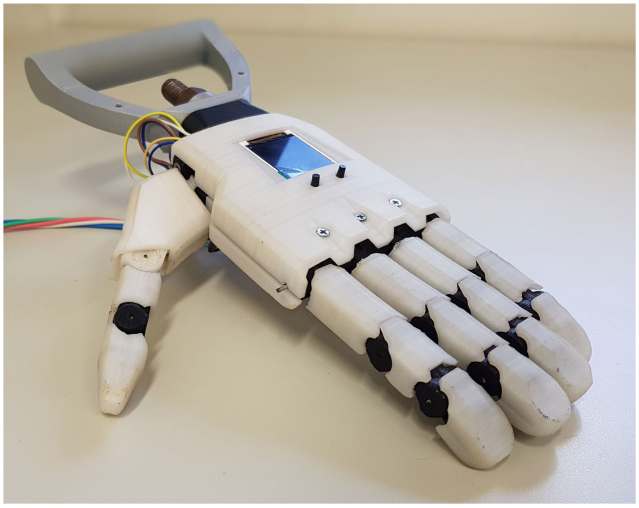

FIGURE 1. The Galileo Hand installed on a probing handle.

availability, pricing and can also offer an extended set of grasps [14]–[16], [18].

The Galileo Hand, shown in Fig. 1, is an affordable, 3D-printed, open-source, anthropomorphic and underactuated myoelectric upper-limb prosthesis for transradial amputees, designed to be easily built and repaired. Its UPI offers a user-friendly alternative to traditional methods. This is achieved by utilizing a reduced muscle contractions subset to gather the user intent, since the bio-potentials of the limb-impaired population differ between themselves and the ones from the healthy subjects, because some of their musculature is uniquely atrophied. In addition to that, it only requires materials that are readily available in developing countries for its construction [17]. Furthermore, the design is intended to be easily integrated on sockets provided by social security entities in underdeveloped countries. This way, both the cost and the manufacturing time are lessened. Moreover, its parametric and modular design allows for an easy modification of the size of the fingers and the palm, with the aim of increasing the range of target users. Furthermore, its six intrinsic actuators and the self-contained embedded controller inside the palm, provide fitting versatility to subjects with different necessities [9], [19].

In order to replicate the six movements of the human thumb (abduction-adduction, flexion-extension and opposition-deposition) [20], [21], a design implementing two actuators has been elaborated. This permits to achieve more customized actions, such as individual finger motions, time-based sequential actions and most common types of grasping based on the Cutkosky grasp taxonomy [22]. Another relevant aspect is that the proposed prosthetic hand weighs under 350g and requires less than $350 to be built.

The rest of this work is structured as follows: Section II elaborates on the state of the art of open-source upper-limb prostheses, as well as their UPIs. Methods involved in the design of the anthropomorphic and under-actuated prosthetic hand are described in Section III. Details about the electrical design, digital signal processing methods employed, as well as the user-prosthesis interface elaborated are described in Sections IV and V, respectively. Additionally, experimental results about the functionality of the system, the strategy of control and the implemented UPI are presented in Section VI. Finally, the conclusions are presented in Section VII.

II. STATE OF THE ART

Traditionally, to analyze the user intent and to activate a specific activation profile, different techniques based on the pre-processing of electromyography (EMG) signals have been the focus of upper-limb prosthesis control research. Nowadays, typical commercial hands are operated by features of a predefined subset of muscle contractions according to a state machine model. Meanwhile, most research prosthetic hands are based on pattern recognition with a multimodal (or hybrid) approach. This method consists in combining the EMG features with information gathered from other sensor types to address some issues that arise while utilizing EMG, such as electrode positioning, fatigue, inherent crosstalk in the surface signal, displacement of the muscles and the limb position effect [10], [11], [23]. Some multimodal works have shown an increase in the classification accuracy by employing EMG in tandem with an Inertial Measurement Unit (IMU) or combining it with mechanomyography (MMG) techniques with successful results, like gathering the features with microphones (mMMG) or accelerometers (aMMG) [24], [25]. Besides, other projects have implemented Optical Fiber Force Myography (FMG) as an affordable and more accurate alternative to the usual non-hybrid versions [26], [27]. In addition to that, ultrasound imaging has also been used to interpret the user's intention; this is called sonomyography (SMG). This method detects the morphological changes of the muscles in the forearm during the performance of different actions and relates them to the wrist's generalized coordinates [28], [29].

On the other hand, these multimodal systems were also introduced to improve the user control of prosthetic devices. Implementing an EMG-Radio Frequency Identification (RFID) hybrid and using RFID tags on specific objects to reduce the cognitive effort to operate a prosthesis has been proposed in [30]. Similarly, other works have experimented with combining EMG systems with voice-control and visual feedback, allowing the users to decide between different modalities to control their prosthetic device [17].

Other approaches utilizing Brain-Machine Interfaces (BMIs) as a means to control upper-limb prostheses have also been proposed. They are based on high-density electrocorticography (ECoG), permitting the user to control each individual finger in a natural way. The main problems with this methodology are its invasiveness and price, because it requires an implant consisting of an ECoG array in the brain and a targeted muscle re-innervation (TMR) on a specific set of muscles, which results in challenging procedures for the amputees [7]. Other studies implemented a combination of BMI with other technologies, like voice recognition, eye tracking and computer vision techniques. Nevertheless, they

required high levels of concentration and training, entailing a massive cognitive effort from the user [31], [32].

Computer vision approaches, like the one-shot learning method, implemented to generate specific grasps for unknown objects, have also been employed to control prosthetic devices. This methodology ''generalizes a single kinesthetically demonstrated grasp to generate many grasps of other objects of different and unfamiliar shapes'' [33]. Additionally, another hybrid control using an augmented reality (AR) headset with an integrated stereo-camera pair was used to activate a prosthetic device via the detection of specific muscle activity. This system is able to provide a suggestion regarding the grasp to be actioned via stereo-vision methods, while the users adjust the gesture selection using the AR feedback. This results in a low effort control and better accuracy [34].

Finally, to increase the functionality of multi-grasping upper-limb prostheses, some studies developed hybrid deep-learning artificial vision systems combined with EMG. Aiming to improve the way that the system interprets the user intent, it associates a subset of objects to a specific kind of grasp based on their geometric properties. The classification task is completed through an object classifier implemented with a convolutional neural network (CNN) [35]–[37].

Meanwhile, regarding the hardware implemented by the diverse commercial and research prostheses, their design may differ in terms of the fingers' structure, actuation method, weight, price, compliance and materials used. Taking into account the last mentioned aspect, one can classify them into 3D printed prostheses and the ones that are constructed utilizing a different material. The main advantage of non-3D-printed designs is the robustness its composition may provide, even if it results in increasing their cost and weight. Delving into some of these versions, there are several different approaches to reduce the increased price and mass; some of them sacrifice functionality and mobility, such as the SensorHand and the Michelangelo prosthetics. In contrast, other iterations favor functionality over aforesaid aspects, like the BeBionic, which achieves a much lower cost than some of its counterparts (an aproximate of $11000), but has a weight above the mean of the human hand's, increasing the fatigue factor [38], [39]. While robustness is a relevant aspect, several 3D-printed prostheses trade some of it off for a more affordable alternative, some ranging in prices around the order of hundreds of dollars. Three-dimensional printing balances affordability and robustness in comparison to other cheaper methods like injection moulding. Additionally, this methodology also permits to customize the design in an easy manner, without altering the manufacturing line process [4].

Furthermore, a classification according to the degrees of actuation (DOA) and freedom (DOF) has been proposed. They can be differentiated in non-tendon-driven and tendon-driven mechanisms. Moreover, the latter can be categorized based on the actuation method (active or passive) and depending on the DOA and DOF ratio. These characteristics influence directly in the price range and functionality of the devices, permitting or not certain biomimetic motions [40].

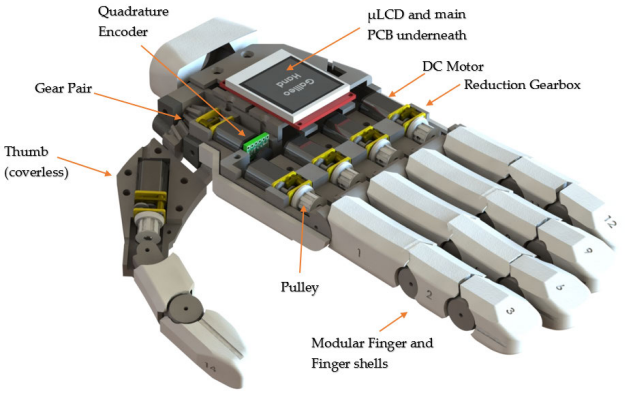

FIGURE 2. Mechanical design of the Galileo Hand.

According to what was enunciated previously, a design that can be replicated using rapid prototyping tools was selected. Thus, the prosthetic hand can be built with different materials, such as Nylon, ABS and PLA polymers, providing a robust and affordable option. Its fingers are assembled via surgical grade elastics and motor-powered waxed strings, providing an under-tendon-actuated system. To operate the device, multimodal approaches can be used due to the flexibility of the controller; however, to gather the user intent, medical grade sEMG electrodes are employed.

III. MECHANICAL DESIGN

The merit of intrinsic actuation pattern (IAP) prosthetic hands is to provide more flexibility for people with different levels of amputation [19], so the project can benefit more users. Since it is essential that the patient's stump plus the prosthesis's span equal the length of the preserved limb so that amputees feel comfortable using it, the prosthesis's size is a relevant aspect. In this way, the placement of the actuators and electronics inside the palm helps achieve symmetry between both arms, regardless of the amputation level, because the prosthesis does not take up space within the socket, which allows for a reduction in length when necessary [19]. Nevertheless, creating an intrinsic design, illustrated in Fig. 2, will increase the mass of the prosthetic hand, which needs to be less than a biological hand's (around 500g), since it will be attached to the softer tissue of the amputated limb instead of being directly attached to the human skeleton, which means that it is perceived heavier by the end user [15].

The prosthesis's proposed design is underactuated with the aim to simplify the manufacturing and assembling processes, as well as to assimilate the human hand's movements and reduce costs. In addition to that, adaptive grasping can be achieved with such actuation system, as explained in [41], [42], which consists in interacting with objects during activities of the daily living (ADLs). The main modules in the prosthesis are the palm, the thumb rotation mechanism, and the fingers, which vary only in the length of each phalanx.

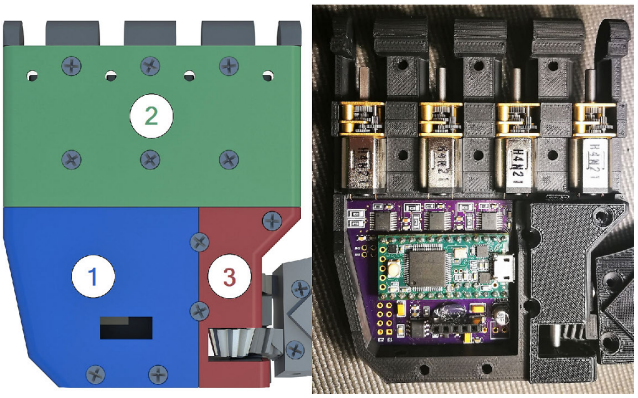

FIGURE 3. Top view of the modular palm sections. (1) The main PCB board controller. (2) Motors driving the index, middle, ring and little fingers. (3) Actuator in charge of the rotation of the thumb.

A. PALM DESIGN AND MECHANISMS

The design requirements were set up with help of two male volunteers suffering from unilateral, transradial amputation and taking into account the results from the reported users' needs in [10]. The mechanism consists in Micro-metal brushed DC gearmotors (250:1) with an output torque of around 0.42 *Nm*, which perform the flexion/extension movements of the five fingers through an under-tendon-actuated system. The palm has three different sections with individual covers, one for the motors powering all digits but the thumb; another for the actuator that enables the thumb rotation; and the last one for the rest of the components; this is shown in Fig. 3. Such a design allows for easy maintenance without disassembling the whole artificial hand.

B. THUMB MOVEMENT CHARACTERISTICS

The thumb has been designed with two DOAs in order to recreate the six movements that humans can perform, as described in [20]. One actuator is located inside the thumb metacarpal phalanx and it is responsible of flexion and extension of the proximal and distal phalanges. The second one, located in the metacarpophalangeal joint of the thumb, is responsible for its abduction and adduction, which is monitored by the reading of a quadrature encoder. This joint is built by a bevel and a helical gear working together to transmit the torque from the actuator with a ratio of 8:11, creating a beveloid gear pair [43], as shown in Fig. 4. Rotating the thumb around an axis shifted 15° from the palm plane increases the abducted position of the thumb. This way, the rotation axis is shifted without the need to incline the motor, allowing it to perform a larger prismatic grasp [22], while, at the same time, saving space inside the palm and making it easier to print.

C. FINGER DESIGN

The remaining fingers consist of three phalanges and three joints, distal and proximal interphalangeal (DIP, PIP) and the metacarpophalangeal (MCP), as shown in Fig. 5. This configuration is meant to mimic the biomechanics of the human hand, resulting in a 15 DOF prosthetic device.

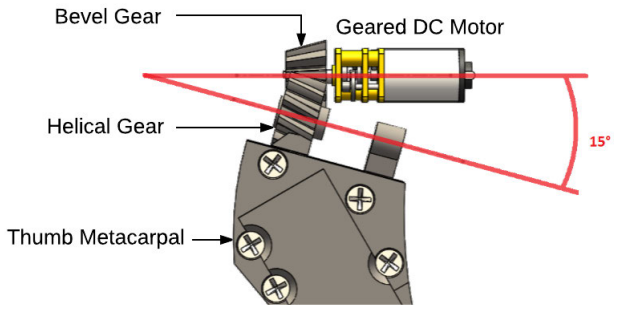

FIGURE 4. Thumb mechanism side view, beveloid gear pair.

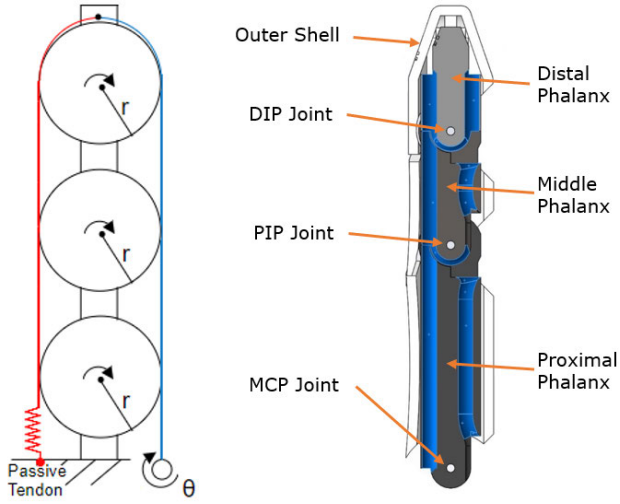

FIGURE 5. Mechanical design for the fingers, where r is the pulley's radius and θ represents the position of the motor.

Additionally, each of their components can be easily reprinted and reassembled using common 3D printing polymers. Moreover, the phalanges were designed to withstand the stress created by the actuators during ADLs. Plus, each finger's outer shell is coupled to their respective phalanx to not only provide a more aesthetic design, but also, offer better grip capabilities if implemented with thermo-flexible materials.

Furthermore, the parametric design of the phalanges allows to modify its length,[1] allowing a wider range of patients to utilize the prosthetic device. With the purpose of creating a more versatile design, fingers can be implemented in both right or left hand prostheses. Moreover, each phalanx and its respective shell are enumerated to simplify the assembly and repairing processes.

The prosthetic device consists in six DOAs, one permitting the thumb's rotation and the other five allow the flexion and extension movements of each finger. These last actions are completed by actuating waxed nylon cords, working as the active tendons; and round surgical elastic cords, as the passive ones. The first, goes through the duct inside the volar face of

[1]The minimal length of the proximal and middle phalanges is 22 *mm*; and 20 *mm* for the distal phalanx, because of the finger-palm ratio restrictions and the PCB size limit.

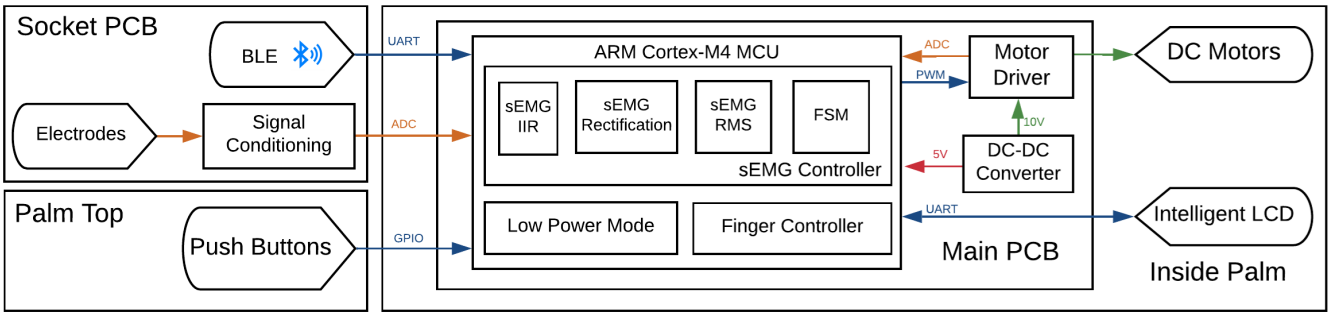

FIGURE 6. System architecture's block diagram illustrating how the components for each module interact with each other.

the finger; and the second one, through the one on the dorsal side, as shown in the blue areas in Fig. 5.

1) UNDER-TENDON-DRIVEN MACHINE

Since each active tendon is driven by a geared DC motor, a positive, active tensile force, f_{ta}, is generated. In contrast, the passive tendon's force, f_{te}, depends uniquely on the deflection of the joints and, to prevent them from loosening, an initial expansion must be considered [40].

Letting L be the number of tendons, N the amount of joints and $\boldsymbol{f}_t = [\, f_{ta} \;\; f_{te} \,]^T$ the resulting tensile force vector, a relationship between $\boldsymbol{f}_t \in \mathbb{R}^L$ and the joint torque vector $\boldsymbol{\tau} \in \mathbb{R}^N$ is given by the equation enounced underneath.

$$\boldsymbol{\tau} = -\mathbf{J}_j^T \boldsymbol{f}_t \tag{1}$$

where $\mathbf{J}_j = \left[\, \mathbf{J}_{ja} \;\; \mathbf{J}_{je} \,\right]^T$ is the Jacobian matrix for the active and passive tendons and, considering r are the radii of the pulleys on each joint, the matrix is given by the following expression.

$$\mathbf{J}_j = \begin{bmatrix} r & r & r \\ -r & -r & -r \end{bmatrix} \tag{2}$$

Alternatively, the tensile force vector for the system can also be defined with the following equation.

$$\boldsymbol{f}_t = \boldsymbol{f}_b - \left(\mathbf{J}_j^T\right)^+ \boldsymbol{\tau} \tag{3}$$

where $\boldsymbol{f}_b \in \mathbb{R}^L$ is a bias tension force vector and $\left(\mathbf{J}_j^T\right)^+$ is the Moore-Penrose pseudoinverse of the matrix $\mathbf{J}_j$ transposed.

Since $\boldsymbol{f}_b$ does not directly affect the joint torque vector, $\boldsymbol{\tau}$, one can define its expression as follows [40].

$$\boldsymbol{f}_b = \mathbf{A}\boldsymbol{\xi}\,, \quad \mathbf{A} = \left[\mathbf{I}_L - (\mathbf{J}_j^T)^+ \mathbf{J}_j^T\right] \tag{4}$$

where $\boldsymbol{\xi}$ is a compatible dimensional vector with the matrix $\mathbf{A}$ and $\mathbf{I}_L$ is the identity matrix of size L.

Therefore, since an initial expansion of the passive tendon is considered for each finger, it is evident that $\boldsymbol{f}_b > 0$, resulting in a tendon-driven machine and, in addition to that, since $\text{rank}(\mathbf{J}_j) = 1 < N$, the system is, additionally, defined as an under-tendon-driven mechanism. With this information,

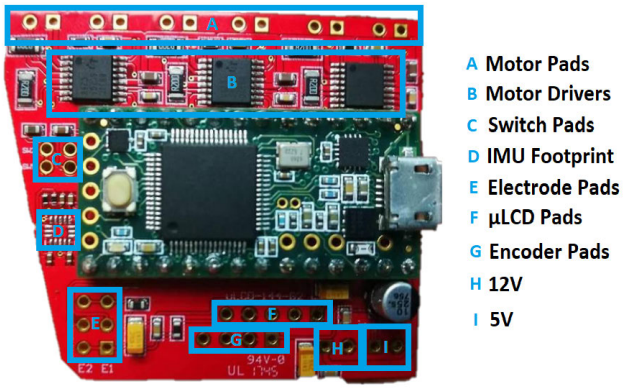

FIGURE 7. Control board PCB based on ARM Cortex-M4.

one can deduce that the system's dynamic with the following equations:

$$\mathbf{M}\ddot{\mathbf{q}} + \left[\frac{1}{2}\dot{\mathbf{M}} + \mathbf{S} + \mathbf{B}_0\right]\dot{\mathbf{q}} + \mathbf{G}_g\mathbf{q} = \boldsymbol{\tau} \tag{5}$$

$$\tau_m = J_m\ddot{\theta} + f_{ta}r_p \tag{6}$$

where $\mathbf{M}$ and $\mathbf{B}_0$ are the inertia and damping matrices of the finger, accordingly, $\mathbf{S}$ is a skew-symmetric matrix and $\mathbf{G}_g$ is the gravity load matrix. Additionally, J_m and b are the gearhead's moment of inertia and friction coefficient, correspondingly; τ_m, the torque exerted by the motor gearhead's shaft; and r_p, the radius of the pulley mounted on it [40].

IV. ELECTRICAL DESIGN

A versatile myoelectric controller is implemented with a low cost and high performance microcontroller unit (MCU) based on the ARM Cortex-M4 architecture on a custom control board (shown in Fig. 7). The SIMD extensions of its instruction set provide it signal processing capabilities and separate stack pointers, which result ideal for real-time applications through the use of Real-Time Operating Systems (RTOS) [44]. In this manner, the MCU can run multiple processes concurrently, allowing scalability, modularity and reliability to the system. Thus, it can easily adapt to different control strategies, as well as different UPIs, providing multiple ways to interpret the user intent through the use of one or more types of transducers, such as in [17], [18], [26], [27], [37].

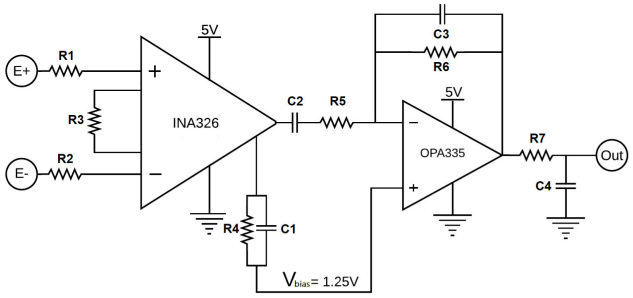

FIGURE 8. Simplified circuit of the sEMG signal conditioning stage, a low-pass active filter.

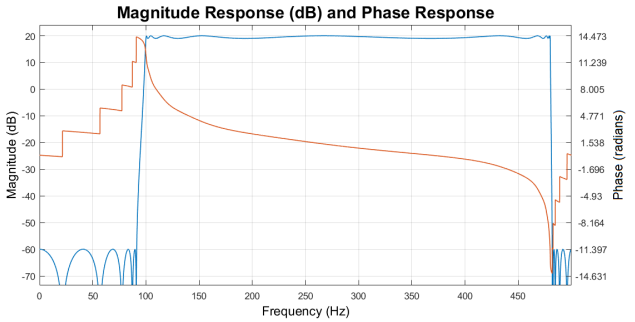

FIGURE 9. Magnitude and phase responses of the IIR band-pass filter, in blue and orange, respectively.

On the other hand, since sEMG is still one of the most reliable methods to activate the functionalities of prosthetic devices (despite of its well-known issues) and, taking into account that it is relatively easy to build or acquire an affordable version of this kind of sensor, three custom PCB boards were designed, the control board and two signal conditioning ones, in order to achieve a self-contained embedded controller that provides fitting versatility to subjects with different amputation degrees. The block diagram proposed, illustrated in Fig. 6, shows the system architecture of the self-contained embedded controller that fits inside the palm of the prosthesis.

However, affordable commercial sensors such as the MyoWare Muscle Sensors (analog interface) or Thalmic Labs' Myo armband (Bluetooth Low Energy) can be easily adapted to the system.

A. sEMG Control Design

A simple on-off sEMG controller based on time-domain features that triggers transitions of a Finite-State Machine (FSM) (in Section V) was designed in order to implement an intuitive user-friendly interface, allowing to achieve more customized hand actions without requiring long periods of training from the user [18].

1) sEMG SIGNAL ACQUISITION AND CONDITIONING

In order to save costs, two affordable, bipolar channels, implemented with nickel-plated copper rivets as surface mounted electrodes, are placed on the palmaris longus and the extensor digitorum muscles (for unilateral below-elbow disarticulations) [16], [17]. Since the biopotentials acquired are about $\pm 25\ \mu V$ to $\pm 10\ mV$, ranging in a bandwidth between 30 Hz to 2 kHz, a signal conditioning stage was implemented. It consists in a single-supply operation, based on the TI INA326 high-performance rail-to-rail precision instrumentation amplifier and a TI OPA335 working together under a first-order, low-pass, active filter configuration, as shown in Fig. 8. In order to collect useful sEMG data from the patient's stump and sense the biopotentials of muscular fibers during different actions, an output signal span in the range of 0 V to 3.3 V and a bandwidth between 0 Hz to 500 Hz was considered [18], [45], [46].

2) sEMG SIGNAL PROCESSING

The digital signal processing (DSP) involved in the sEMG controller is implemented on a custom, main PCB board based on the Teensy 3.2 development board (PJRC), using NXP's ARM Cortex-M4 Kinetis K20 microcontroller. There, two channels of sEMG signals are collected using the on-chip ADC with 1 kHz of sample rate. Then, they are filtered in order to eliminate the interference caused by the mains power line's AC frequency, using an Infinite Impulse Response (IIR) Elliptic Band-Pass Filter of order 20 with a pass-band from 100 Hz to 480 Hz and quantized for single precision. The filter was implemented using the transposed direct form II biquadratic IIR filter structure from the CMSIS-DSP API for ARM Cortex-M MCUs [47], [48]. Frequency and phase response, as well as the Pole/Zero plot of the IIR filter are shown in Figs. 9 and 10, respectively.

3) sEMG ON-OFF TIMING DETECTION

A single-threshold method is used to detect the "on" and "off" timing of each muscle. Then, sEMG data collected from each channel, k, in a time window of 50 ms, is operated according to Eq. 7, so the mean absolute value μ_k is determined. Later, it is compared to a predefined threshold, α_k, which varies between users and depends on the mean power of the background noise of each channel [49], [50].

As shown in Eq. 8, if this threshold is exceeded, a contraction q_k is detected and a transition in the UPI's FSM (Fig. 12) is triggered [17], [51].

$$\mu_k = \frac{1}{N}\sum_{n=1}^{N} |x_{k,n}| \tag{7}$$

where $x_{k,n}$ is the sample n from the channel k, and N is the size of the collected window.

$$q_k = \begin{cases} 1, & \mu_k \geq \alpha_k \\ 0, & \mu_k < \alpha_k \end{cases} \tag{8}$$

B. MOTOR CONTROL DESIGN

Three H-bridge drivers, TI DRV8833, were selected to drive each of the six brushed DC motors actuating the fingers. This selection was based on their pin requirements and through

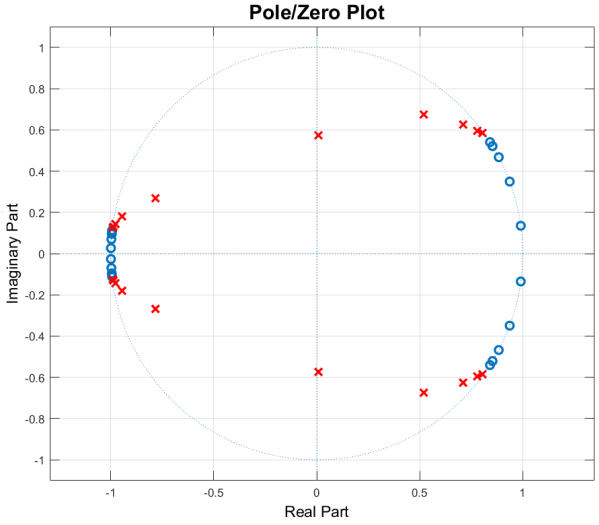

FIGURE 10. Pole-Zero plot showing the stability of the IIR elliptic band-pass filter.

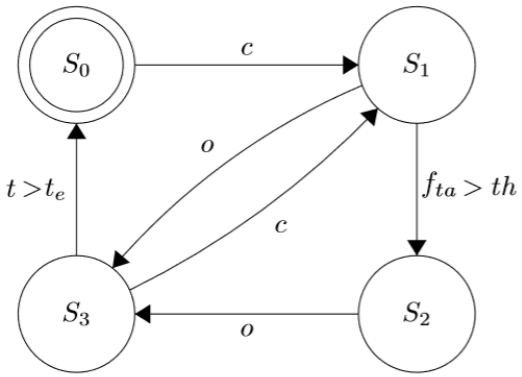

FIGURE 11. FSM demonstrating the opening/closing behaviour of each finger on the prosthesis.

complementary PWM, they provide active braking, speed and direction control. This way, the prosthesis is able to perform predefined gestures through a PI controller to rotate the thumb and a hybrid on-off control system (shown in Fig. 11), to limit the finger's tensile force.

This last one was designed taking into account that the gearhead on the motor introduces backlash and friction to the system, but, because of the power transmitted by the gearbox, each finger acts similarly to a non-backdrivable system. That is why the on-off controller was implemented to achieve the flexion/extension movements with the necessary force to hold different objects, which is the same as f_{ta}. Considering the equation (1) and the system (5)-(6), one can limit it according to the following expressions in a simplified model, i.e. by considering the current demanded by the motor, i_a, and the nominal torque at the gearhead, τ_m.

$$f_{ta} = \frac{Gk_t i_a - J_m \ddot{\theta}}{r_p} \tag{9}$$

where G is the gearbox's ratio and k_t is the motor's torque constant.

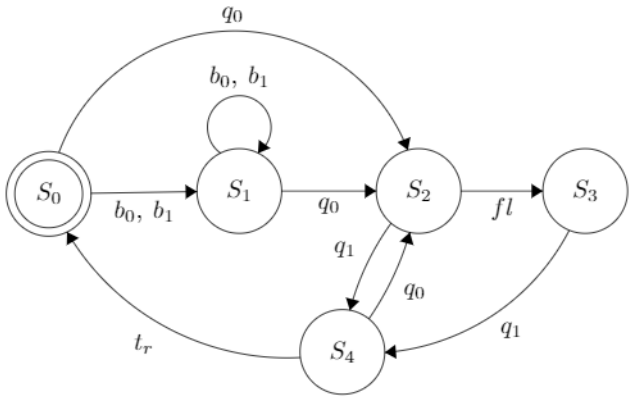

FIGURE 12. FSM illustrating the behavior of the interface using a multimodal approach with buttons and sEMG sensors.

With this information, the threshold th for each finger was determined experimentally. Thus, the high-level controller (in Fig. 11) results in the following: the system starts with the finger fully extended (in an "open" position), modelled by the state S_0. The transition to S_1 happens when the command to move the finger, c, is received, activating the motor and causing the finger to flex. During this process, the RMS value of the current is monitored by the MCU and it is used to obtain the force equivalent to limit it to th; if it is exceeded, then the switch to S_2 happens. The exact value of the threshold may be different for each individual finger, as each one has different size and, therefore, different mechanical characteristics, so this procedure was carried out experimentally. At this point, the finger is considered to have reached its final position and will start to reopen if another command, o, is issued by the user, as shown by the transition from S_2 to S_3. The transition to S_0 is time-based and t_e is about 1.5 times less than the time taken to finish said action (the time spent in S_1). This discrepancy arises, because of the elastic installed on each member of the prosthetic limb, since the material opposes itself to the coiling process, but favors the uncoiling one. Furthermore, t_e was measured experimentally (as shown in Fig. 16) and represents the time it takes to fully extend each finger. It is relevant to note that the closing/opening processes may be interrupted and reversed if the appropriate commands are received.

V. USER-PROSTHESIS INTERFACE

To select a UPI for the prosthesis, both interfaces used for previous versions of the Galileo Hand were evaluated to determine which one provided a better user experience. Since both of them were implemented with the same hardware (shown in Fig. 1), the tests run did not possess any bias involving price ranges or physical characteristics, like general aesthetics, weight, amount of DOF and DOA, as well as the sensor used to detect the user intent. For the sake of these trials, the signal capture system selected was the Myo armband (because of its comfort and easy installation on the volunteers), which was placed on each of the subjects'

forearms (on the same arm as the Galileo Hand to create a natural operation mode), where the stump for transradial amputees is located. Also, a limited contractions subset was aimed for to interact with the prosthesis, since some of the gestures can not be performed by the limb-impaired, while, at the same time, providing a decent amount of actions at their disposal.

A. INTERFACES CONSIDERED

Hereunder, the different UPIs taken into account are elaborated on.

1) sEMG PATTERN RECOGNITION

The first interface, based on [17], but employing the Myo's pattern recognition methods, one of the more traditional research alternatives [11], consists in a simplistic system that maps each of the predefined ''Myo poses'' to a gesture to be executed. The mapping was carried out as follows: ''wave in'' (flexing the hand) to a pointing position; ''wave out'' (hand extension) to carry out a lateral grasp; ''double tap'' (two swift, consecutive contractions) to a hooking stance; while ''fist'' and ''fingers spread'' to closing and opening all fingers, respectively. The gestures selected were the ones considered to be the most useful in the ADLs.

2) MULTIMODAL APPROACH USING BUTTONS AND MYO INTERFACE

The functionality for this version, similar to the work presented in [18], is illustrated in the FSM in Fig. 12. The muscle contractions subset, $Q = \{q_0, q_1\}$, corresponding to the hand extension and flexion movements, respectively, and the buttons set, $B = \{b_0, b_1\}$, are used to operate the prosthesis. Using b_0 and b_1 alters the position forwards or backwards in the menu displayed on a μLCD screen (as shown in Fig. 13), accordingly. These changes take place in the state S_1, indicating that an alteration in the screen's state is occurring. Such changes are blocked to the user the moment an action is active, because the timing for operating the motors differs between actions, so, if an action were changed while another is active, this could lead to wrong finger positioning.

On the other hand, S_0 indicates that the prosthesis is resting in its default state, the fingers on the prosthesis are fully extended; while S_3, that the fingers are flexed according to the selected action. Moreover, S_2 and S_4 indicate that the prosthetic hand is currently closing or opening, respectively, processes that can be interrupted by each other if a correct command is received. Additionally, to activate an action, q_0 needs to be received; however, if q_1 is detected, the gesture deactivation process begins.

Other relevant elements in the FSM representing the interface's behavior are the flags fl and t_r. The first one informs that all the fingers have reached their desired position when performing an action, while the second represents that the time required to fully open the hand has passed.

FIGURE 13. Graphical menu on the screen mounted on the prosthetic device (left) and the Galileo Hand performing a power grip on a ball (right).

B. NASA TASK LOAD INDEX EVALUATION

To effectively determine how amiable the interfaces are, a NASA Task Load Index (TLX) test was carried out, not unlike [52], and compared the results to each other.

This scale quantifies the effectiveness and performance of the workload to operate the device, taking the following categories into account: mental, physical and temporal demands, performance, effort needed to interact with the prosthesis and the frustration its utilization evokes.

The selection of this scale to valuate the interfaces was based on requiring a user testing, post-task evaluation method, since post-test assessment techniques (like SUS), do not permit to rate each part of the interfaces separately. Plus, methods like SEQ are not as thorough as the one implemented, since not many categories are considered during experimentation, providing a more binary result. Additionally, the test chosen has numerous research and industry benchmarks to interpret the scores in context, which can be helpful for future works.

The trials were carried out according the Ethical Committee recommendations (CAAE 58592916.9.1001.5404) and were passed to 10 volunteers, who were asked to rate each category in a scale from 1 to 20. The volunteers consisted in 8 male and 2 female subjects between the ages of 22 and 35, without any physical impairment. The evaluation and comparison processes were carried out for the two UPIs previously mentioned to notice the strengths and weaknesses of each iteration and find the superior one.

The test consisted in performing different actions with the Galileo Hand to interact with their environment and try some of the expressions at their disposal. The evaluation consisted in executing the following gestures: ''Close'' (flexing all fingers), ''Peace'' (only the index and middle finger remain extended), ''Rock'' (all fingers are closed, but the index and the little finger) and ''Three'' (the index, middle and annular fingers are the only ones in an open position). Later, the volunteers were asked to hold a wallet, a bottle and to press a specific key in a computer keyboard (similar to the actions illustrated in Fig. 14). The tasks were repeated thrice for the subjects to properly adapt to the operation mode.

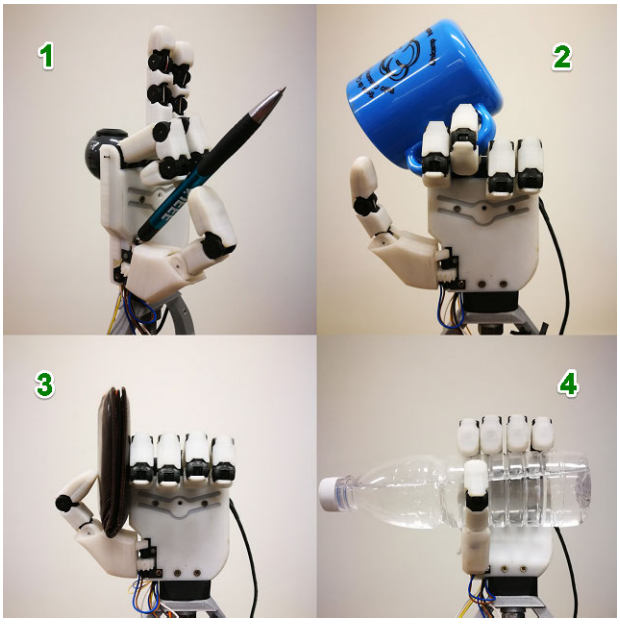

FIGURE 14. Galileo Bionic Hand performing different grasps helpful for ADLs. (1) Precision (2) Hook (3) Lateral (4) Power.

VI. RESULTS

Since the prosthesis has to be able to enclose the control board, together with the μLCD and the DC motors, the minimization of the palm is restricted. Considering this, its minimal size is 98 $mm \times 69.6\ mm \times 25\ mm$. In a similar sense, to avoid a disproportional hand, the fingers' length was also limited, 22 mm for the middle and proximal phalanges; and 20 mm for the distal ones. Moreover, the total weight of the prosthetic hand lingers under 350g, excluding the socket and the alternative chosen for powering it up, which does not have to be placed on the patient's stump. This fulfills the requirement of not being too heavy for the user to feel uncomfortable, when installing the assistive device on soft tissue.

Furthermore, other relevant aspects to mention are the reaction times and general capacities of the system. The MCP joint's minimum flexion and extension times are around 800 ms and 600 ms, respectively. Similarly, the thumb MCP joint's abduction and adduction lowest times remain near 150 ms. Additionally, each finger can hold up to a maximum of 2.5 kg with a driven motor, as shown in Fig. 15, where it was taken to its braking point; and 5 kg, when the actuator is inoperative. Besides, the resulting force exerted with the power grasp has a magnitude of 50 N.

Moreover, the experimentation for the determination of the threshold to restrain the strength of the finger, th, consisted in displaying the current demanded by the motor, i_a, as well as the gearhead's angular position, θ, during the closing and opening processes. This resulted in the graphs shown in Fig. 16, where the peaks shown in the second image reflect an alteration in the actuator's behavior, i.e. when the motor starts moving or is shut down. Here, one can notice that a less than 10 ms latency exists between both graphs.

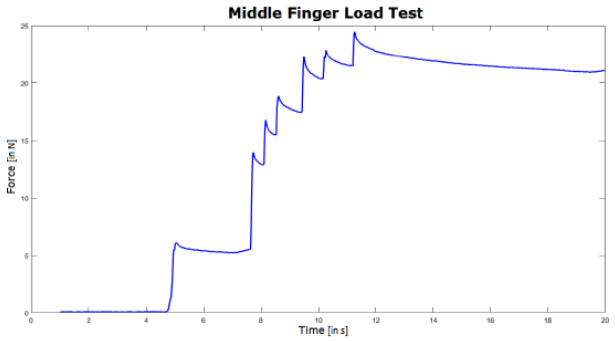

FIGURE 15. Load testing results for a driven middle finger, where it was brought to its breaking point to determine the maximum weight it can hold.

Furthermore, the peaks overcoming the set threshold for the current (marked in red in the second graph of Fig. 16), indicate the moment the digit starts and finishes flexing, respectively. At the latter point, the motor is shut down to save energy, but the finger remains closed, because the passive tendon's force does not overcome the nominal torque at the gearhead output. The aforementioned limit was selected so that the actuators do not turn off when other peaks occur, i.e. when turning the motor on for the uncoiling process. This lead to setting this restraint to different values for each finger, according to each of their mechanical properties and the desired force the user wants to exert with them, f_{ta}. It is relevant to note that the first peak is ignored when evaluating this condition, since it means the motor is starting. However, this is not a problem when the extension process begins, as the elastic favors this movement, so less power is demanded. On the other hand, it is also relevant to note the overall lack of noise of the system in terms of the current, however an IIR low pass filter could be implemented to mitigate its effects.

In addition to that, with the resulting behavior of the gearhead's angular position, it was possible to determine the finger extension time, t_e, as utilized in the FSM in Fig. 11. This was possible by measuring the relationship between the flexion and extension times for the digits, which resulted in a factor of around 1.5.

On the other hand, the results for the NASA TLX experiment are shown in Fig. 17, where each bar represents how each individual subject rated the interfaces for each category in question. Their means are visualized in Fig. 18 along with their standard deviations. The figures reflect a great discrepancy in most categories, except for the performance.

The version consisting in the direct mapping of the actions shows the best results in physical and temporal demand, as well as the effort required to complete a task, while the multimodal one resulted in the least frustrating interface and the one requiring less mental demand. Both iterations excel in diverse aspects, but a clear improvement between them is not palpable with the previous graph. Therefore, an overall performance statistic was elaborated (Fig. 19), which shows an average of all six categories for all versions. They display

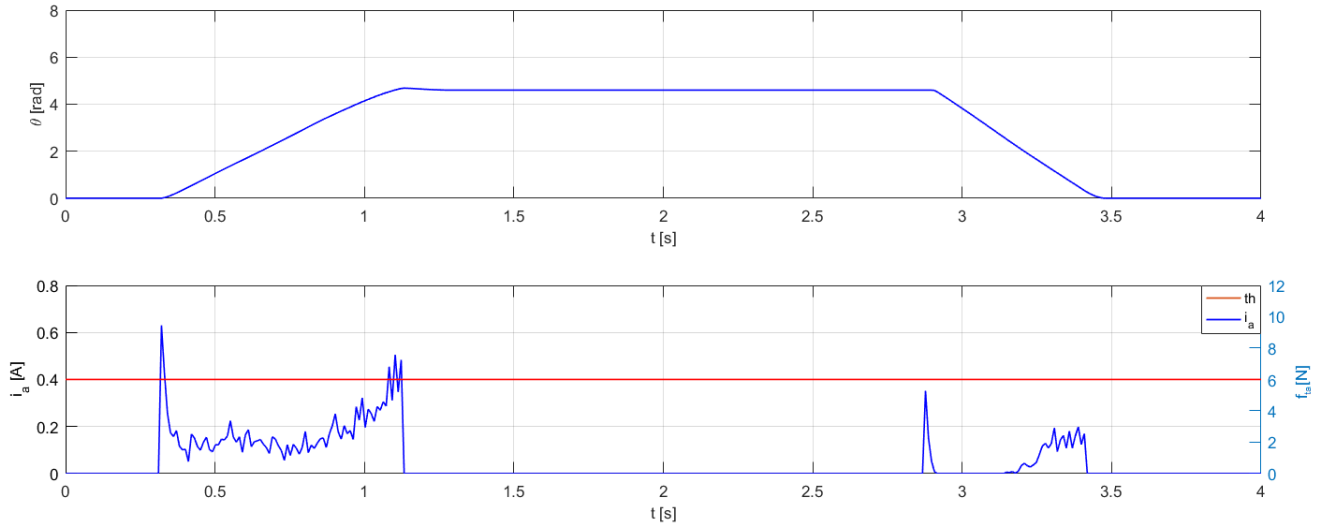

FIGURE 16. The angular position's behaviour for the opening and closing processes for the middle finger is shown on the uppermost graph, together with the one for the current (and active tension force), on the lowermost one, together with their corresponding thresholds.

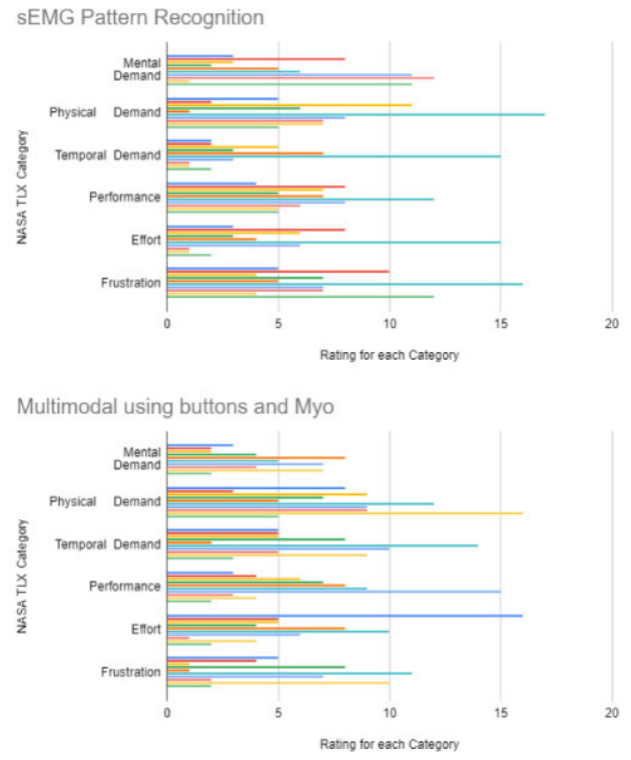

FIGURE 17. NASA TLX results for both UPIs evaluated. Results for each of the ten volunteers are represented by same-colored bars on each category.

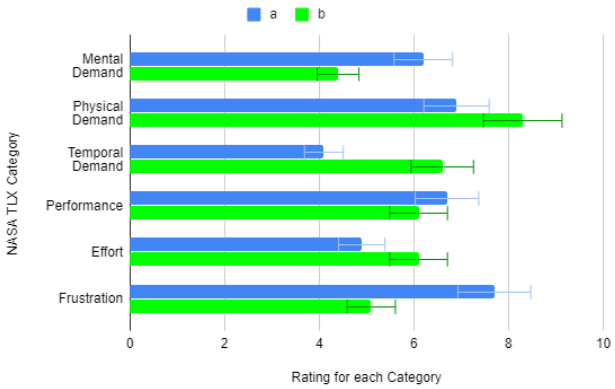

FIGURE 18. Mean and standard deviation of the results gathered from the volunteers' evaluation. Where (a) is the sEMG Pattern Recognition one and (b) the one using the multimodal interface.

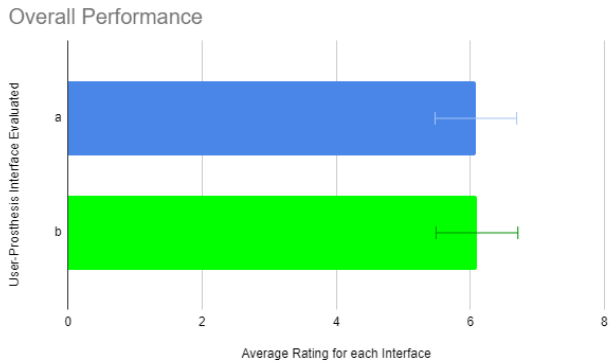

FIGURE 19. Overall performance of both interfaces. (a) is the version using the sEMG patter recognition interface and (b) is the multimodal one.

similar user-friendly behaviors around the upper 70% with respect to NASA TLX's scale.

Since the means for both versions are very similar ((a) has a mean of 6.08; and (b) one of 6.1), a Factorial Analysis of Variance (ANOVA) test was run on the results to verify if the discrepancy between both results is relevant. The F statistic obtained was 3.84, when its critical value is 0.0005, considering an alpha of 0.05. This affirms the main effect hypothesis, showing an insignificant inequality between both interaction processes, resulting in equally amiable interfaces.

So, in conclusion, the interface that does not use the buttons proved to be the less physically demanding version, which may lie in the swift selection of actions allowed by the lack of a menu to interact with, resulting, also, in requiring a lower level of effort to operate. However, although insignificant, a slight inferiority was palpable in comparison to the alternative. This can be the consequence of the need to memorize the actions mapped to the Myo default poses, which does not come naturally to the subjects, as they need to be focused on the tasks at hand, which may explain the elevated mental demand and frustration observed in the rating process.

In opposition, the lack of frustration for the multimodal iteration may be result of the alternative to navigate along the menu using the buttons, since the Myo classification process has been known to misinterpret certain actions at times. In addition to that, an aspect noted after performing these trials was that a multimodal approach implementing a system using an extended contractions subset did not result in a relevant improvement. However, since both versions showed similar results, it is convenient to provide the patient with a larger gamut of actions to provide a more customized and practical prosthetic device, although increasing the price slightly, which still remains under the $350 mark, it still proves to be a much more affordable alternative than typical commercial products. It is relevant to note that this price includes the PCB, 3D-printing materials, electronic components and a power source.

VII. CONCLUSION

An affordable and functional upper-limb prosthesis for transradial amputees was successfully tested and validated. In addition to that, since its weight remains under the average human hand's, its usability over long periods of time is favored. Moreover, regarding the operational aspect of the Galileo Hand, it is relevant to note the swift responsiveness of the on-off sEMG controller, which can be observed in Fig. 16, as it possesses a latency, which is barely, if at all, noticed by the user. Also, its modular, intrinsic and versatile design allows for its adaptation to the user's needs, such as providing alternate ways of gathering the user intent. Furthermore, since the system is an under-tendon-driven machine, the mechanism is underactuated while still allowing for an efficient gripper and maintaining a low cost, because it requires less actuators than alternate systems. Its grip feasibility was validated through the tests performed by the volunteers when interacting with arbitrary objects in a successful manner, as shown in Fig. 14. Additionally, it was also proven that the maximum force exerted by each finger is enough to accomplish common ADLs.

Finally, based on the NASA TLX scale (as shown in Fig. 19), the proposed UPI has been shown to be user-friendly and also allows to increase the amount of customized hand postures that can be performed; an aspect commonly lacking in many other prosthetic devices, even though it is an important one, as it permits its operation by people with diverse levels of amputation. Additionally, this UPI only needs the detection of two contractions, which were selected so that they can be easily performed by users with transradial amputations, by the sEMG system. However, these results have to be juxtaposed to the ones gathered by tests run on a relevant sample of physically impaired subjects.

REFERENCES

[1] D. Pilling, P. Barrett, and M. Floyd, *Disabled People and the Internet: Experiences, Barriers and Opportunities*. London, U.K.: Univ. London, 2004.

[2] *World Report on Disability: World Health Organization*, World Health Org., Geneva, Switzerland, 2011.

[3] D. Cummings, "Prosthetics in the developing world: A review of the literature," *Prosthetics Orthotics Int.*, vol. 20, no. 1, pp. 51–60, Apr. 1996.

[4] J. ten Kate, G. Smit, and P. Breedveld, "3D-printed upper limb prostheses: A review," *Disab. Rehabil., Assistive Technol.*, vol. 12, no. 3, pp. 300–314, Apr. 2017.

[5] M. M. Bridges, M. P. Para, and M. J. Mashner, "Control system architecture for the modular prosthetic limb," in *Johns Hopkins APL Tech. Dig.*, 2011, vol. 30, no. 3, pp. 217–222.

[6] T. J. Levy and J. D. Beaty, "Revolutionizing prosthetics: Neuroscience framework," in *Johns Hopkins APL Tech. Dig.*, 2011, vol. 30, no. 3, pp. 223–229.

[7] G. Hotson, D. P. Mcmullen, M. S. Fifer, M. S. Johannes, K. D. Katyal, M. P. Para, R. Armiger, W. S. Anderson, N. V. Thakor, B. A. Wester, and N. E. Crone, "Individual finger control of a modular prosthetic limb using high-density electrocorticography in a human subject," *J. Neural Eng.*, vol. 13, no. 2, Apr. 2016, Art. no. 026017.

[8] C. Cipriani, M. Controzzi, and M. C. Carrozza, "Objectives, criteria and methods for the design of the SmartHand transradial prosthesis," *Robotica*, vol. 28, no. 6, pp. 919–927, Oct. 2010.

[9] C. Cipriani, M. Controzzi, and M. C. Carrozza, "The SmartHand transradial prosthesis," *J. NeuroEng. Rehabil.*, vol. 8, no. 1, p. 29, 2011.

[10] F. Cordella, A. L. Ciancio, R. Sacchetti, A. Davalli, A. G. Cutti, E. Guglielmelli, and L. Zollo, "Literature review on needs of upper limb prosthesis users," *Frontiers Neurosci.*, vol. 10, p. 209, May 2016.

[11] A. Fougner, O. Stavdahl, P. J. Kyberd, Y. G. Losier, and P. Parker, "Control of upper limb prostheses: Terminology and proportional myoelectric control-A review," *Trans. Neural Syst. Rehabil. Eng.*, vol. 20, no. 5, pp. 663–677, 2012.

[12] C. Medynski and B. Rattray, "Bebionic prosthetic design," in *Proc. Myoelectric Symp.*, Fredericton, NB, Canada, 2011, pp. 279–282.

[13] C. Connolly, "Prosthetic hands from touch bionics," *Ind. Robot, Int. J.*, vol. 35, no. 4, pp. 290–293, Jun. 2008.

[14] G. P. Kontoudis, M. V. Liarokapis, A. G. Zisimatos, C. I. Mavrogiannis, and K. J. Kyriakopoulos, "Open-source, anthropomorphic, underactuated robot hands with a selectively lockable differential mechanism: Towards affordable prostheses," in *Proc. IEEE/RSJ Int. Conf. Intell. Robots Syst. (IROS)*, Sep. 2015, pp. 5857–5862.

[15] P. Slade, A. Akhtar, M. Nguyen, and T. Bretl, "Tact: Design and performance of an open-source, affordable, myoelectric prosthetic hand," in *Proc. IEEE Int. Conf. Robot. Autom. (ICRA)*, May 2015, pp. 6451–6456.

[16] A. Akhtar, K. Y. Choi, M. Fatina, J. Cornman, E. Wu, J. Sombeck, C. Yim, P. Slade, J. Lee, J. Moore, D. Gonzales, A. Wu, G. Anderson, D. Rotter, C. Shin, and T. Bretl, "A low-cost, open-source, compliant hand for enabling sensorimotor control for people with transradial amputations," in *Proc. 38th Annu. Int. Conf. IEEE Eng. Med. Biol. Soc. (EMBC)*, Aug. 2016, pp. 4642–4645.

[17] J. Fajardo, A. Lemus, and E. Rohmer, "Galileo bionic hand: SEMG activated approaches for a multifunction upper-limb prosthetic," in *Proc. IEEE 35th Central Amer. Panama Conv. (CONCAPAN XXXV)*, Nov. 2015, pp. 1–6.

[18] J. Fajardo, V. Ferman, A. Lemus, and E. Rohmer, "An affordable open-source multifunctional upper-limb prosthesis with intrinsic actuation," in *Proc. IEEE Workshop Adv. Robot. Social Impacts (ARSO)*, Mar. 2017, pp. 1–6.

[19] H. Liu, D. Yang, S. Fan, and H. Cai, "On the development of intrinsically-actuated, multisensory dexterous robotic hands," *ROBOMECH J.*, vol. 3, no. 1, p. 1, Dec. 2016.

[20] I. Kapandji, *The Physiology of the Joints: Upper Limb*, vol. 1. London, U.K.: Churchill Livingstone, 2007, pp. 1–372.

[21] M. M. Rahman, T. T. Choudhury, S. N. Sidek, and A. Awang, "Mathematical modeling and trajectory planning of hand finger movements," in *Proc. 1st Conf. Syst. Informat., Modeling Simulation*, 2014, pp. 43–47.
[22] M. R. Cutkosky, "On grasp choice, grasp models, and the design of hands for manufacturing tasks," *IEEE Trans. Robot. Autom.*, vol. 5, no. 3, pp. 269–279, Jun. 1989.
[23] A. Fougner, E. Scheme, A. D. C. Chan, K. Englehart, and Ø. Stavdahl, "Resolving the limb position effect in myoelectric pattern recognition," *IEEE Trans. Neural Syst. Rehabil. Eng.*, vol. 19, no. 6, pp. 644–651, Dec. 2011.
[24] W. Guo, X. Sheng, H. Liu, and X. Zhu, "Mechanomyography assisted myoeletric sensing for upper-extremity prostheses: A hybrid approach," *IEEE Sensors J.*, vol. 17, no. 10, pp. 3100–3108, May 2017.
[25] S. Wilson and R. Vaidyanathan, "Upper-limb prosthetic control using wearable multichannel mechanomyography," in *Proc. Int. Conf. Rehabil. Robot. (ICORR)*, Jul. 2017, pp. 1293–1298.
[26] E. Fujiwara, Y. T. Wu, C. K. Suzuki, D. T. G. de Andrade, A. R. Neto, and E. Rohmer, "Optical fiber force myography sensor for applications in prosthetic hand control," in *Proc. IEEE 15th Int. Workshop Adv. Motion Control (AMC)*, Mar. 2018, pp. 1–6.
[27] J. Fajardo, A. R. Neto, W. Silva, M. Gomes, E. Fujiwara, and E. Rohmer, "A wearable robotic glove based on optical FMG driven controller," in *Proc. IEEE 4th Int. Conf. Adv. Robot. Mechatronics (ICARM)*, Jul. 2019, pp. 81–86.
[28] Y. P. Zheng, M. M. F. Chan, J. Shi, X. Chen, and Q. H. Huang, "Sonomyography: Monitoring morphological changes of forearm muscles in actions with the feasibility for the control of powered prosthesis," *Med. Eng. Phys.*, vol. 28, no. 5, pp. 405–415, Jun. 2006.
[29] A. S. Dhawan, B. Mukherjee, S. Patwardhan, N. Akhlaghi, G. Diao, G. Levay, R. Holley, W. M. Joiner, M. Harris-Love, and S. Sikdar, "Proprioceptive sonomyographic control: A novel method for intuitive and proportional control of multiple degrees-of-freedom for individuals with upper extremity limb loss," *Sci. Rep.*, vol. 9, no. 1, pp. 1–15, Dec. 2019.
[30] M. S. Trachtenberg, G. Singhal, R. Kaliki, R. J. Smith, and N. V. Thakor, "Radio frequency identification-an innovative solution to guide dexterous prosthetic hands," in *Proc. Annu. Int. Conf. IEEE Eng. Med. Biol. Soc.*, Aug. 2011, pp. 3511–3514.
[31] C. M. Oppus, J. R. R. Prado, J. C. Escobar, J. A. G. Marinas, and R. S. J. Reyes, "Brain-computer interface and voice-controlled 3D printed prosthetic hand," in *Proc. IEEE Region 10 Conf. (TENCON)*, Nov. 2016, pp. 2689–2693.
[32] D. P. Mcmullen, G. Hotson, K. D. Katyal, B. A. Wester, M. S. Fifer, T. G. McGee, A. Harris, M. S. Johannes, R. J. Vogelstein, A. D. Ravitz, W. S. Anderson, N. V. Thakor, and N. E. Crone, "Demonstration of a semi-autonomous hybrid brain–machine interface using human intracranial EEG, eye tracking, and computer vision to control a robotic upper limb prosthetic," *IEEE Trans. Neural Syst. Rehabil. Eng.*, vol. 22, no. 4, pp. 784–796, Jul. 2014.
[33] M. Kopicki, R. Detry, M. Adjigble, R. Stolkin, A. Leonardis, and J. L. Wyatt, "One-shot learning and generation of dexterous grasps for novel objects," *Int. J. Robot. Res.*, vol. 35, no. 8, pp. 959–976, Jul. 2016.
[34] M. Markovic, S. Dosen, C. Cipriani, D. Popovic, and D. Farina, "Stereovision and augmented reality for closed-loop control of grasping in hand prostheses," *J. Neural Eng.*, vol. 11, no. 4, 2014, Art. no. 046001.
[35] G. Ghazaei, A. Alameer, P. Degenaar, G. Morgan, and K. Nazarpour, "Deep learning-based artificial vision for grasp classification in myoelectric hands," *J. Neural Eng.*, vol. 14, no. 3, Jun. 2017, Art. no. 036025.
[36] N. Bu, Y. Bandou, O. Fukuda, H. Okumura, and K. Arai, "A semi-automatic control method for myoelectric prosthetic hand based on image information of objects," in *Proc. Int. Conf. Intell. Informat. Biomed. Sci. (ICIIBMS)*, Nov. 2017, pp. 23–28.
[37] J. Fajardo, V. Ferman, A. Munoz, D. Andrade, A. R. Neto, and E. Rohmer, "User-prosthesis interface for upper limb prosthesis based on object classification," in *Proc. Latin Amer. Robotic Symp., Brazilian Symp. Robot. (SBR) Workshop Robot. Edu. (WRE)*, Nov. 2018, pp. 390–395.
[38] A. Saenz. *How Much is the Newest Advanced Artificial Hand? $11;000 USD (Video)*. [Online]. Available: https://singularityhub.com/2010/06/30/how-much-is-the-newest-advanced-artificial-hand-11000-usd-video/
[39] J. T. Belter, J. L. Segil, A. M. Dollar, and R. F. Weir, "Mechanical design and performance specifications of anthropomorphic prosthetic hands: A review," *J. Rehabil. Res. Develop.*, vol. 50, no. 5, p. 599, 2013.
[40] R. Ozawa, K. Hashirii, and H. Kobayashi, "Design and control of underactuated tendon-driven mechanisms," in *Proc. IEEE Int. Conf. Robot. Autom.*, May 2009, pp. 1522–1527.
[41] T. Takaki and T. Omata, "High-performance anthropomorphic robot hand with Grasping-Force-Magnification mechanism," *IEEE/ASME Trans. Mechatronics*, vol. 16, no. 3, pp. 583–591, Jun. 2011.
[42] P. Dario, C. Laschi, M. C. Carrozza, E. Guglielmelli, G. Teti, B. Massa, M. Zecca, D. Taddeucci, and F. Leoni, "An integrated approach for the design and development of a grasping and manipulation system in humanoid robotics," in *Proc. IEEE/RSJ Int. Conf. Intell. Robots Syst. (IROS)*, vol. 1, Nov./Oct. 2000, pp. 1–7.
[43] C. Zhu, C. Song, T. C. Lim, and S. Vijayakar, "Geometry design and tooth contact analysis of crossed beveloid gears for marine transmissions," *Chin. J. Mech. Eng.*, vol. 25, no. 2, pp. 328–337, Mar. 2012.
[44] M. Gouda, "CMSIS-RTOS an API interface standard for real-time operating systems," in *Proc. ARM Technol. Symp.*, 2012, pp. 5–16.
[45] M. Rossi, S. Benatti, E. Farella, and L. Benini, "Hybrid EMG classifier based on HMM and SVM for hand gesture recognition in prosthetics," in *Proc. IEEE Int. Conf. Ind. Technol. (ICIT)*, Mar. 2015, pp. 1700–1705.
[46] S. Benatti, B. Milosevic, F. Casamassima, P. Schonle, P. Bunjaku, S. Fateh, Q. Huang, and L. Benini, "EMG-based hand gesture recognition with flexible analog front end," in *Proc. IEEE Biomed. Circuits Syst. Conf. (BioCAS) Proc.*, Oct. 2014, pp. 57–60.
[47] H.-P. Huang and C.-Y. Chiang, "DSP-based controller for a multi-degree prosthetic hand," in *Proc. ICRA. Millennium Conf. IEEE Int. Conf. Robot. Automat. Symp.*, vol. 2, Apr. 2000, pp. 1378–1383.
[48] J. Yiu, *The Definitive Guide to ARM CORTEX-M3 and CORTEX-M4 Processors*, 3rd ed. Amsterdam, The Netherlands: Elsevier, 2014, ch. 22.
[49] M. B. I. Reaz, M. S. Hussain, and F. Mohd-Yasin, "Techniques of EMG signal analysis: Detection, processing, classification and applications," *Biol. Procedures Online*, vol. 8, no. 1, pp. 11–35, Dec. 2006.
[50] C. J. De Luca, "The use of surface electromyography in biomechanics," *J. Appl. Biomech.*, vol. 13, no. 2, pp. 135–163, May 1997.
[51] E. N. Kamavuako, E. J. Scheme, and K. B. Englehart, "Determination of optimum threshold values for EMG time domain features; a multi-dataset investigation," *J. Neural Eng.*, vol. 13, no. 4, Aug. 2016, Art. no. 046011.
[52] D. Andrade, A. R. Neto, and E. Rohmer, "Human prosthetic interaction: Integration of several techniques," in *Proc. Simpsio Brasileiro De Automao Inteligente*, 2017, pp. 1–7.

JULIO FAJARDO received the B.S. degree in electrical and computer engineering and the M.S. degree in industrial electronics from Galileo University Guatemala City, Guatemala, in 2012 and 2015, respectively. He is currently pursuing the Ph.D. degree in electrical engineering with the State University of Campinas (UNICAMP), Campinas, São Paulo, Brazil.

From 2013 to 2017, he was a Research Assistant with the Turing Research Laboratory, FISICC, Galileo University. His research interest includes assistive robotics specially focused on upper-limb prostheses and orthoses, robust control applied to robotics by the use of linear matrix inequalities, digital signal processing and machine learning techniques to interpret the user intent through electromyography, force myography, and near-infrared spectroscopy signals.

VICTOR FERMAN received the B.S. degree in mechatronics engineering and the M.S. degree in industrial electronics from Galileo University, Guatemala City, Guatemala, in 2015. He is currently pursuing the Ph.D. degree in electrical engineering with the State University of Campinas (UNICAMP), Campinas, São Paulo, Brazil.

From 2015 to 2017, he worked as a Research Assistant with the Turing Research Laboratoty, FISICC, Galileo University. His research interests include assistive robotics focused on upper-limb prostheses, human–machine interface, and gait control for lower-limb exoskeletons.

DIEGO CARDONA received the B.S. degree in electrical and computer engineering from the Galileo University, Guatemala City, Guatemala, in 2020.

He is currently a Research and Development Assistant with the Turing Laboratory, Galileo University. His work has been focused on PCB design, embedded systems in upper-limb prostheses, and the way these devices are meant to interact with the users.

GUILLERMO MALDONADO is currently pursuing the B.S. degree in mechatronics engineering from Galileo University, Guatemala. He is also working with the Turing Research Laboratory, as a Research assistant, mainly on the research and development of prosthetic hands, their mechanic designs and intricacies, and 3D printing.

ALI LEMUS received the master's degree in applied information sciences from the University of Tohoku, Japan, in 2009. He was a Computer Science Engineer with Universidad Francisco Marroquin, in 2002, and a Researcher in artificial intelligence and neural networks with the Intelligent Nano Integration Systems, Japan, in 2007. He was the Director of the Research and Development, Computer Science Department, Galileo University, in 2011, the Turing Laboratory, in 2013. He was a Co-Founder Elemental Geeks, in 2011. His special fields of interest included machine learning, e-learning, education, MOOCs, gamification, and games.

ERIC ROHMER received the Ph.D. degree from Tohoku University, Japan, in 2005. He worked as a Robotic Researcher with Tohoku University, until 2011. He is currently a Professor and a Robotic Researcher with the Faculty of Electrical and Computation Engineering, State University of Campinas, Brazil. He is also a Co-Founder of the Brazilian Institute of Neurosciences and Neurotechnologies (BRAINN). His field of interest concerns dynamic simulation based telerobotic platforms, mobile robots' locomotion for space exploration and search and rescue operations, and assistive and rehabilitation robotics focusing on mobility and upper limbs assistance. He is also one of the researchers who designed and developed Quince robot, the first Japanese robot in use inside the Fukushima crippled nuclear reactor.